PHYSICAL REVIEW B VOLUME 38, NUMBER 14 15 NOVEMBER 1988-I

Kinetics of H_2 passivation of P_b centers at the (111) Si-SiO_2 interface

K. L. Brower
Sandia National Laboratories, Albuquerque, New Mexico 87185-5800

(Received 8 June 1988)

This paper is concerned with the determination of the kinetic parameters and the chemical reactions that characterize the passivation of P_b centers with molecular hydrogen. P_b centers are paramagnetic defects at the (111) Si-SiO_2 interface. In this study P_b centers associated with thermal oxides grown on (111) silicon substrates at 850 °C were measured with electron paramagnetic resonance. We observe that the P_b resonance appears to be unaffected by subsequent *in situ* vacuum anneals for temperatures up to at least 850 °C. The passivation of P_b centers with H_2 occurs for temperatures above approximately 220 °C; dissociation of passivated centers in vacuum occurs for temperatures in excess of 550 °C. The rate of passivation of P_b centers with H_2 is proportional to the H_2 concentration and the density of P_b centers at the interface and is characterized by the forward rate constant k_f. The temperature dependence of k_f is observed to obey the Arrhenius equation and is characterized by an activation energy of 1.66 ± 0.06 eV and a preexponential factor, k_{0f}, of $1.94^{+2.00}_{-1.00}\times10^{-6}\ \mathrm{cm^3/sec}$. The rate equation for passivation of P_b centers with H_2 is consistent with a chemical process in which a hydrogen molecule reacts directly with a P_b center. The rate at which this chemical reaction occurs is consistent with the diffusion of the H_2 molecule among the accessible interstices of the SiO_2 and the reaction site at P_b centers. We also observe that the spin-lattice relaxation time, T_1, for P_b centers at low temperatures (<100 K) increases with decreasing oxide thicknesses (<800 Å). T_1 also increases if the dry thermal oxides are annealed in H_2 between 225 and 575 °C or cooled in Ar gas after thermal oxidation.

I. INTRODUCTION

Dry thermal oxidation of (111) silicon results in the growth of SiO_2 on silicon. The interface between the crystalline silicon and the oxide is typically atomically abrupt and flat over long distances.[1-4] Ordinarily, the [111] Si bonds perpendicular to the (111) surface adjacent to the thermal oxide are believed to be covalently bonded to oxygen atoms of the thermal oxide. Observation of this material system with electron paramagnetic resonance (EPR) reveals the presence of a distinct interface defect called the P_b center.[5] The paramagnetism of this interface defect arises from an unpaired electron in a nonbonding [111] sp^3-like hybrid orbital localized on a surface Si atom[6-8] presumedly due to a missing oxygen atom.[6,7,9] Up to approximately 0.5% of the surface silicon atoms are the site of P_b centers which are neutrally charged, paramagnetic, and nonbonding after thermal oxidation. The physical process by which the P_b centers are formed remains unknown. The P_b center can lose or gain an electron depending upon the position of the Fermi level in the silicon band gap.[10-13] Electrical measurements indicate that the P_b center is also the dominant charge trap at the Si-SiO_2 interface;[10,12] therefore, it is also of technological concern and importance. The molecular and electronic structure of the P_b center, as deduced primarily from magnetic resonance[14] and theoretical[15-17] studies, suggest that it should be chemically active by virtue of its dangling-bond character.[18] Previous EPR studies indicate that the P_b resonance is affected by annealing in hydrogen.[5,7,19,20]

As a charge trap the P_b center can be eliminated by passivating it with hydrogen, although this solution may be the source of other problems in a radiation environment. Thus, understanding passivation on the atomic scale is important with respect to understanding the nature of the process and its limitations. The P_b center is not readily eliminated by vacuum annealing. We have observed in connection with this work that P_b centers are stable under vacuum annealing to temperatures up to at least 850 °C.[21] We suspect that unless one is careful, false thermal annealing effects of the P_b center can conceivably arise from impurity contamination. The passivation process is believed to involve the binding of a hydrogen atom to the trivalent silicon atom, resulting in the formation of a diamagnetic, neutral defect symbolized as HP_b. P_b centers can be passivated with H_2 above approximately 220 °C; however, passivated P_b centers dissociate in vacuum at temperatures in excess of approximately 550 °C.[19] As a result of dissociation in vacuum, the P_b center reappears as observed by EPR with the apparent liberation of the hydrogen.

In this paper a kinetic model is developed from our experimental results for the rate at which P_b centers are passivated with molecular hydrogen as a function of H_2 pressure, annealing time, and temperature. From the temperature dependence of the rate at which P_b centers are passivated, we deduce the activation energy for passivation of P_b centers with molecular hydrogen. The dominant chemical process by which P_b centers are passivated with H_2 is identified from an analysis of the reaction kinetics. This model also considers the trapping characteristics of the H_2 molecule at the P_b reaction site.

Our experimental approach is presented in Sec. II. In addition to our kinetic results, qualitative effects due to thermal oxidation and annealing under various gas ambients on the EPR measurements as well as the spin-lattice relaxation rate at low temperatures of the P_b centers are presented in Sec. II. In Sec. III we discuss three thermochemical effects, namely the thermal stability, and the hydrogen passivation and dissociation of the P_b center, which are important in this study. The quantitative aspects of the kinetic model for the passivation process are developed in Sec. IV. Here, consideration of the solubility of molecular hydrogen in the thermal oxide as well as its rate of diffusion is taken into account. The results of our experimental measurements and the analysis of our data in terms of the kinetic equations are presented in Sec. V. In Sec. VI we identify a chemical and kinetic process which is consistent with our experimental observations. Our conclusions are presented in Sec. VII.

II. EXPERIMENTAL TECHNIQUES

A. Sample preparation

In our experimental approach thin silicon samples 75 μm thick (or less) and having a (111) surface area of 2.26×23.24 mm^2 were fabricated from an ingot of intrinsic, float-zone silicon (p type, 2000 Ω cm). Each sample was oriented such that the broad face (2×23 mm^2) was a (111) plane, the 23-mm edge was a $[11\bar{2}]$ direction, and the 2-mm edge was a $[1\bar{1}0]$ direction. Before thermal oxidation approximately 500–1000 Å of silicon were removed by a white etch.[22]

These samples were subsequently oxidized in dry flowing oxygen at a pressure of 760 Torr at 850 °C. Oxide thicknesses ranged from 300 to 1200 Å depending on the time allotted for thermal oxidation. During oven warm-up the samples were in vacuum ($<1\times10^{-6}$ Torr).[23] Oxidation and annealing were achieved using a tubular furnace mounted on a track that allows it to be moved in relation to the single-wall, fixed fused-silica tube that runs through the center of the furnace. After oxidation the sample tube was evacuated (1×10^{-6} Torr) and the furnace was offset from the samples. The samples were allowed to cool to room temperature (≈23 °C) and remained in vacuum. Next, the furnace was reheated to the anticipated anneal temperature and then recentered over the samples. For studies on the hydrogen passivation of P_b centers, the samples were annealed in H_2 (99.999% pure) under specified conditions of time, temperature, and H_2 pressure.[24] After annealing in hydrogen for a specified period of time, the passivation process was halted by removing the hydrogen. The furnace was then removed from the samples and they were allowed to cool in vacuum to room temperature. Each data point (Sec. V, Figs. 1–7) corresponds to one sample prepared as just described; samples were not subsequently repassivated for subsequent data points. The samples were later removed and exposed to air (~20 min) while being mounted for EPR measurements. We have subsequently observed that the intensity of the P_b resonance is unaffected by storage at room temperature in a nitrogen atmosphere for periods of time extending to at least 6 months.

B. Measurement techniques

The interfacial area of our EPR samples was maximized by stacking 10 oxidized samples together, forming a sample bundle which was mounted on the axis of our TE_{011} cylindrical microwave cavity (cavity diameter = cavity height = 19.3 mm). The (111) Si-SiO_2 interface area within the microwave cavity was typically 9 cm^2. The effects of P_b centers associated with sample edges are automatically excluded in our measurements because they are at a different magnetic field.

These samples were measured with a K-band superheterodyne spectrometer at 273 K using narrow-band lock-in detection in the absorption mode in slow passage.[25] The resonances were observed at microwave power levels for which no saturation occurred (-20 dB m in this case) and magnetic field modulation levels for which the signal response was linear. The signal-to-noise ratio in these measurements was enhanced by signal-averaging 25 sweeps of the spectrum and subsequent digital filtering.[26] The peak-to-peak height of the derivative of the absorption signal was taken as the relative intensity of the P_b resonance. We are able to measure the relative intensity of the P_b resonance from sample to sample to within approximately ±5%.

C. Other effects

One might think that it would be better to make the EPR measurements at low temperatures since the paramagnetism would be enhanced by the Boltzmann factor. Also, one would have the advantage of a higher loaded cavity Q since any substrate carriers would tend to be frozen out. Measurements were, in fact, begun at 20 K. For thermal oxides annealed in hydrogen between 225 and 575 °C we observed that the spin-lattice relaxation times at 20 K increased to such an extent that it was impossible to measure the residual P_b resonance without saturation. These results suggest that annealing in hydrogen may affect the phonon density of states of the oxide.

Microwave saturation effects of the P_b resonance also indicate that the spin-lattice relaxation times of the P_b resonance increase as the oxide thickness decreases (for oxides less than approximately 800 Å). Although the P_b center is primarily localized on the silicon side of the interface,[16] its spin-lattice relaxation rate at low temperatures (≤100 K) appears to be strongly affected by the properties of the thermal oxide. This effect might be due to significant changes in the density of phonon states in the oxide as the thickness of the oxide is reduced below 800 Å.

To avoid the effects of saturation of the P_b resonance at 20 K associated with thin oxides which have also been annealed in hydrogen, we found it necessary to make EPR measurements above 200 K (Sec. II B).

If one attempts to avoid the saturation problem by growing thicker oxides for measurements at low temperatures, another problem becomes important. Thicker dry oxides necessitate oxide growth at higher temperatures (> 900 °C) and longer times. Such samples cause a degradation in loaded cavity Q and a corresponding lost of sensitivity. We suspect that in this case a significant number of shallow thermal donor levels are formed in the silicon substrate during the oxidation process, giving rise to carriers that are not frozen out at liquid-He temperatures.[27] At room temperature the overall sensitivity of our spectrometer with these samples is too low for meaningful measurements.

We also observe that dry thermal oxides subsequently allowed to cool from the growth temperature in Ar gas have relatively long spin-lattice relaxation times.[8] High-temperature postanneals in ammonia (850 or 1050 °C) or nitrogen do not appear to significantly alter the spin-lattice relaxation rates at 20 K. In the case of the 850-°C ammonia anneals the oxide next to the silicon is believed to be nitrogen rich;[28] however, this effect has no apparent effect on the spin-resonance spectrum of the P_b centers. Thus, we conclude that although various processing procedures may not change the molecular or electronic structure or the density of P_b centers, alterations in the local environment can affect their low-temperature spin-lattice relaxation rates.

Finally, we also noticed that the noise level of our spectrometer was anomalously high with some samples. We theorized that this was due to electrical breakdown or gradual dissipation of trapped charge or static charge associated with the oxide. The noise would be due to the interaction between the charged carriers associated with the electrical breakdown process and the electromagnetic field within the microwave cavity. This effect is also especially noticeable with Si_4N_3 samples which are well known for their charge trapping.[29] In these cases the samples in our microwave cavity were in a vacuum of approximate 10^{-1} Torr. We observed that exposure to approximately 10–20 Torr of He gas quenched this source of noise. We suspect that the He gas, which could easily permeate the SiO_2,[30] was capable of either being ionized or bearing charge and thus neutralizing charged regions of the oxide.

III. THERMOCHEMICAL EFFECTS

In our initial experiments we monitored the effects of annealing thermal oxides in various ambients (vacuum, ammonia, forming gas—10 at. % H_2, 90 at. % N_2, and some noble gases). Only those gases with a hydrogen component passivated the P_b center under certain annealing conditions. Consequently, we proceeded to use pure hydrogen in our experiments in order to perform the experiments under the simplest possible conditions. We now briefly summarize the effects of H_2 annealing on P_b centers.

(1) After thermal oxidation of (111) Si, which results in the formation of P_b centers at the (111) Si-SiO_2 interface, we observe that the density of these defects is unaffected by subsequent thermal anneals in vacuum.[21] This effect is observed for annealing temperatures extending up to at least 850 °C. Thus, P_b centers *appear* to be thermally stable for temperatures up to at least 850 °C. This suggests that the changes due to annealing in hydrogen, for example, are due to chemical changes rather than just thermal annealing effects.

This is an interesting result in light of the fact that radiation-induced dangling-bond defects within bulk silicon, such as the divacancy, anneal out at approximately 175 °C.[31] The thermal stability of the P_b center suggests that P_b centers do not migrate on the (111) Si-SiO_2 interface. Also, there is a strong tendency for impurities, oxygen in particular, to be incorporated into vacancy structures.[32] It is surprising that the P_b center, which has been characterized as a vacancy defect, exhibits structural stability at elevated temperatures. The structural stability of the P_b center suggests that the dry thermal oxide and the crystalline silicon in the region of the interface are devoid of mobile impurities which might otherwise react chemically with the P_b center.

(2) The intensity of the P_b spectrum is observed to decrease if the thermally oxidized silicon samples are annealed in molecular hydrogen between typically 220 and at least 500 °C. This effect is attributed to a hydrogen atom becoming chemically bound to the P_b center, thereby converting the paramagnetic, neutral P_b center to a diamagnetic, neutral HP_b defect. One objective of this paper is to develop a kinetic model for this passivation process and to determine the kinetic parameters which characterize the rate at which the passivation process proceeds (see Sec. V). The results of our EPR measurements indicate that the time rate of change in the surface density of P_b centers due to the effects of annealing in molecular hydrogen is proportional to the molecular hydrogen concentration in the thermal oxide and the surface density of P_b centers (Sec. IV). The constant of proportionality, k_f, is observed to be temperature dependent and is shown to obey the Arrhenius relationship.

(3) Passivated P_b centers (HP_b) are diamagnetic and unobservable with EPR; however, the P_b spectrum does reappear after annealing such samples in vacuum above 550 °C. It is believed that the P_b spectrum reappears as a result of the dissociation of the H atom from the passivated P_b center. The determination of the kinetic parameters which characterize this process are the subject of a planned forthcoming paper.

IV. KINETICS OF PASSIVATION

Although one can conceive of various mechanisms for the way in which the passivation of P_b centers with molecular hydrogen proceeds (Sec. VI), the following kinetic equation has been found to be consistent with our experimental data. The time rate of change in the interfacial density of P_b centers is described by the rate equation

$$\frac{d[P_b]}{dt} = -k_f[H_2][P_b] \tag{1}$$

for temperatures at least between 230 and 260 °C and for which the dissociation process is negligible. Equation (1) indicates that the rate at which the surface density of P_b

centers decreases due to the passivation process is proportional to the volume concentration of H_2 at the interface, $[H_2]$, the surface density of P_b centers, $[P_b]$, and the forward rate constant, k_f, which is temperature dependent. Thus, the solution to Eq. (1) for the case in which the interfacial density of P_b centers is initially N_0 is

$$[P_b]=N_0\exp(-k_f[H_2]t)\ . \qquad (2)$$

The forward rate constant, k_f, at each temperature can be deduced by analyzing experimental data taken under the appropriate experimental conditions using Eqs. (2).

It is essential to know the concentration of H_2 at the Si-SiO_2 interface since the rate of passivation of P_b centers is directly proportional to the H_2 concentration at the Si-SiO_2 interface [Eq. (1)]. The hydrogen in our experiments is believed to reach the region of the interface by the diffusion of H_2 through the thermal oxide.[33]

Shelby has plotted the diffusion constant of D_2 in bulk vitreous silica between 278 and 356 K.[33] The diffusion constant for chemically inert atoms or molecules in glasses is accurately given by the equation

$$D=D_0T\exp(-E/kT)\ . \qquad (3)$$

According to the classical theory of reaction rates, the diffusion constant for H_2 at any given temperature is the square root of the D/H mass ratio times the diffusion constant of D_2 at that temperature in the same material.[34] The activation energy for the diffusion of H_2 (or D_2) in vitreous silica is 0.386 eV, and the value for D_0 in Eq. (3) is 3.10×10^{-7} (2.19×10^{-7}) $cm^2/K\,sec$ for H_2 (D_2) for temperatures at least between 278 and 356 K. Thus, the rapidity of H_2 diffusion in vitreous SiO_2 is such that in the case of a 500-Å-thick thermal oxide the concentration of H_2 at the interface reaches 84% of the dissolved concentration of H_2 at the surface in 1 sec at room temperature; at 250 °C, the H_2 concentration equilibrates within about 1 msec.

The rate at which the H_2 concentration equilibrates is orders of magnitude faster than the rate of H_2 passivation of P_b centers in our sample processing. We do not believe that the rate at which the $[H_2]$ equilibrates is reduced significantly by chemical absorption of the H_2 by the SiO_2. The chemical solubility of H_2 in vitreous silica dominates above 600 °C.[35] Also, the work of Myers[36] indicates that the temperature threshold for the trapping of hydrogen in thermal oxides is between 200 and 300 °C. Because the $[H_2]$ equilibration time is so short for our samples, the effects of any hydrogen trapping within the bulk of the oxide on the H_2 concentration at the interface are neglected in our kinetic model.

The value for $[H_2]$ which we have used in Eq. (2) corresponds to the physical solubility of H_2 in vitreous silica. For low pressures the solubility of H_2 in vitreous silica, C_0, is proportional to the gaseous H_2 pressure, p, at the surface and has been given by Shelby[33] as

$$C_0=K(T)pV^{-1}\ , \qquad (4)$$

where $K(T)$ is specified by the expression[30]

$$K(T)=\left[\frac{h^2}{2\pi mkT}\right]^{3/2}\left[\frac{1}{kT}\right]\left[\frac{\exp(-h\nu/2kT)}{1-\exp(-h\nu/kT)}\right]^3 \times\exp(-\varepsilon/kT)\ . \qquad (5)$$

The parameter, V^{-1}, in Eq. (4) is the concentration of sites into which molecular hydrogen dissolves in vitreous silica and has a value of 1.27×10^{21} sites/cm^3.[33] For a glass the value of V^{-1} depends on the size of the atomic species. The vibration frequency, ν, corresponds to 4.1×10^{12} Hz for H_2 and 3.13×10^{12} Hz for D_2 in vitreous SiO_2.[33] The binding energy, ε, for a molecule of hydrogen of mass m to a SiO_2 surface site is -0.105 eV,[33] and corresponds to the heat of absorption at the surface.

V. EXPERIMENTAL RESULTS AND ANALYSIS

The results of our EPR measurements are presented in Figs. 1–7, where the intensity of the P_b resonance is plotted versus annealing time. We have basically three sets of data. The data in Figs. 1 and 2 are for different H_2 pressures with constant annealing temperature and oxide thickness; Figs. 3–5 pertain to different annealing temperatures with constant H_2 pressure and oxide thickness. The data in Figs. 5–7 are for different oxide thicknesses and constant temperature and H_2 pressure. The straight line in each of Figs. 1–7 corresponds to a least-squares fit of Eq. (2) to the experimental data points; the H_2 concentration needed in Eq. (2) was determined as discussed in Sec. IV. The negative of the slope of these straight lines corresponds to the forward rate constant, k_f, and is tabulated in Table I for each set of data.

Let us consider the pressure effects. Our kinetic model is based on the idea that the rate of passivation is proportional to the H_2 concentration in the oxide at the interface. Our analysis using Eq. (2) of the experimental data in Figs. 1 and 2 gives the same forward rate constant within experimental error for H_2 passivation at pressures of 50 and 190 Torr. We are also able to determine from the experimental data in Figs. 3–5 the forward reaction rate, k_f, at 260 °C and 760 Torr of H_2 (Table I, data set 8)

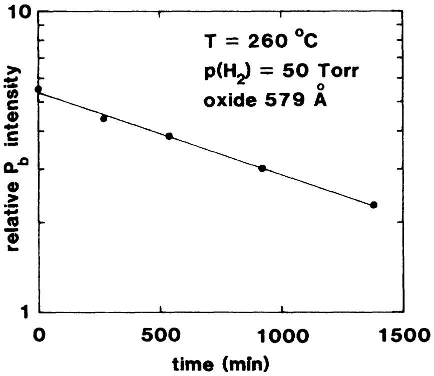

FIG. 1. Plot of the relative intensity of the P_b center vs annealing time. The effects of thermal annealing in pure H_2 at 50 Torr and 260 °C.

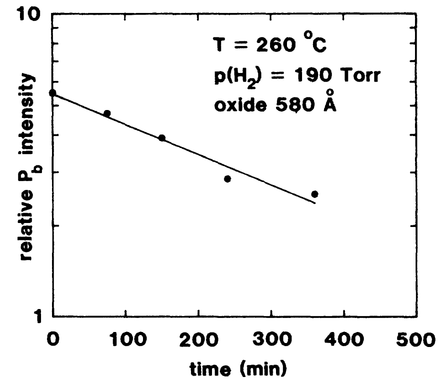

FIG. 2. Plot of the relative intensity of the P_b center vs annealing time. The effects of thermal annealing in pure H_2 at 190 Torr and 260 °C.

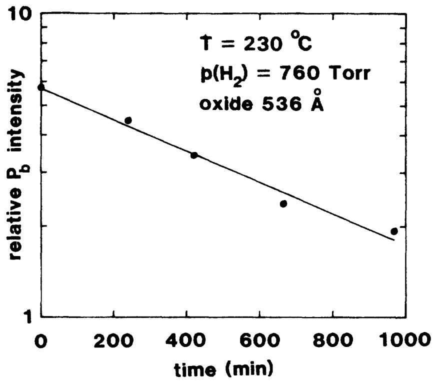

FIG. 5. Plot of the relative intensity of the P_b center vs annealing time. The effects of thermal annealing in pure H_2 at 760 Torr and 230 °C.

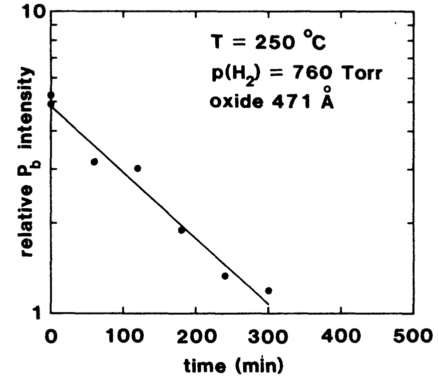

FIG. 3. Plot of the relative intensity of the P_b center vs annealing time. The effects of thermal annealing in pure H_2 at 760 Torr and 250 °C.

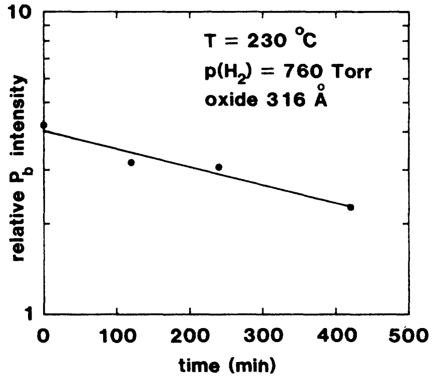

FIG. 6. Plot of the relative intensity of the P_b center vs annealing time. The effects of thermal annealing in pure H_2 at 760 Torr and 230 °C of a thin dry oxide.

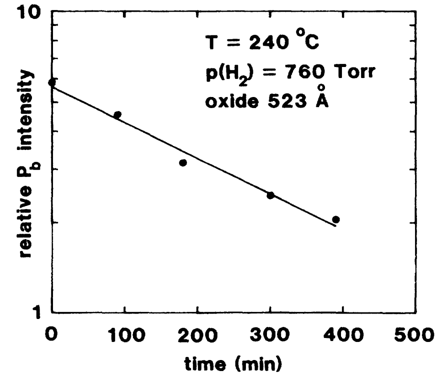

FIG. 4. Plot of the relative intensity of the P_b center vs annealing time. The effects of thermal annealing in pure H_2 at 760 Torr and 240 °C.

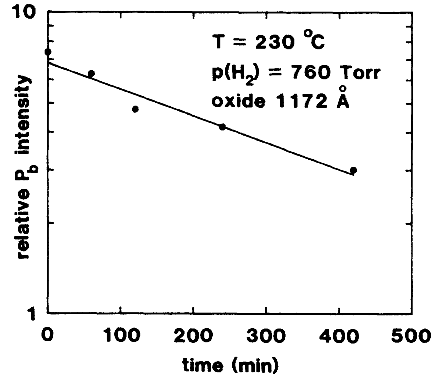

FIG. 7. Plot of the relative intensity of the P_b center vs annealing time. The effects of thermal annealing in pure H_2 at 760 Torr and 230 °C of a thick dry oxide.

TABLE I. Tabulated of the forward rate constant, k_{0f}, as a function of temperature, H_2 pressure, H_2 concentration in the oxide, and oxide thickness. Each k_f is deduced from a least-squares fit of the data in the respective figure to Eq. (2) along with the standard deviation in k_f.

Data set	T (°C)	$p(H_2)$ (Torr)	$[H_2]$ (cm^{-3})	Oxide thickness (Å)	k_f (cm^3/sec)	$\pm\Delta k_f$ (cm^3/sec)	Comments
1	260	50	2.65×10^{16}	579	3.95×10^{-22}	2.92×10^{-23}	Fig. 1
2	260	190	1.01×10^{17}	580	3.84×10^{-22}	3.03×10^{-23}	Fig. 2
3	250	760	4.16×10^{17}	471	2.01×10^{-22}	7.19×10^{-24}	Fig. 3
4	240	760	4.31×10^{17}	523	1.06×10^{-22}	6.39×10^{-24}	Fig. 4
5	230	760	4.47×10^{17}	536	4.44×10^{-23}	2.56×10^{-24}	Fig. 5
6	230	760	4.47×10^{17}	316	5.10×10^{-23}	6.07×10^{-24}	Fig. 6
7	230	760	4.47×10^{17}	1172	7.60×10^{-23}	5.84×10^{-24}	Fig. 7
8	260	760	4.02×10^{17}	$\simeq$510	4.11×10^{-22}	2.0×10^{-23}	Deduced from data in Figs. 3–5 using Eq. (6)

ture dependence of k_f obeys the Arrhenius relationship as shown below. These forward rate constants, k_f, are plotted as a function of H_2 pressure in Fig. 8. The fact that this analysis yields forward rate constants independent of the H_2 pressure to within experimental error indicates that we have determined the correct pressure dependence in our kinetic model [e.g., Eq. (1)].

The forward rate constants tabulated in Table I are plotted in Fig. 9 as a function of $1/T$ and independent of $[H_2]$. Since the passivation process is believed to be a thermally activated process, we have least-squares-fitted the Arrhenius equation,

$$k_f = k_{0f}\exp(-E_f/kT) , \tag{6}$$

to the first five k_f in Table I as a function of temperature. The results of this least-squares analysis gives the straight line in Fig. 9. This analysis indicates that the activation energy, E_f, for the passivation of P_b centers with molecular hydrogen is 1.66±0.06 eV and the preexponential factor, k_{0f}, is $1.94^{+2.00}_{-1.00}\times10^{-6}$ cm^3/sec for temperatures at least between 230 and 260 °C.

The data in Table I indicate that k_f depends weakly on the oxide thickness (data sets 5–7). These data were acquired for several reasons. First, we wanted to verify that k_f was not limited by the rate of diffusion of H_2 to the interface which would cause k_f to decrease monotonically with increasing oxide thickness. Second, we considered the possibility that H_2 might undergo partial chemical absorption of H_2 into the SiO_2 network with the release

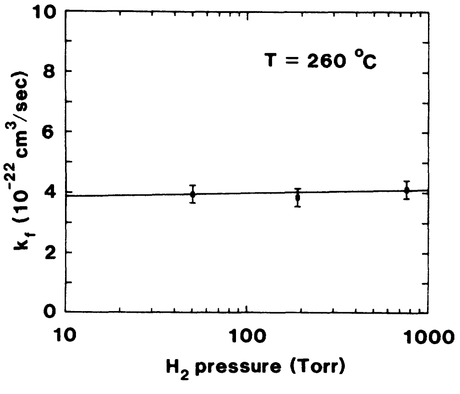

FIG. 8. Plot of the forward reaction rate, k_f, defined in Eq. (2) as a function of the H_2 pressure at 260 °C. The data points with error bars correspond to data in Table I at 260 °C and H_2 pressures of 50, 190, and 760 Torr.

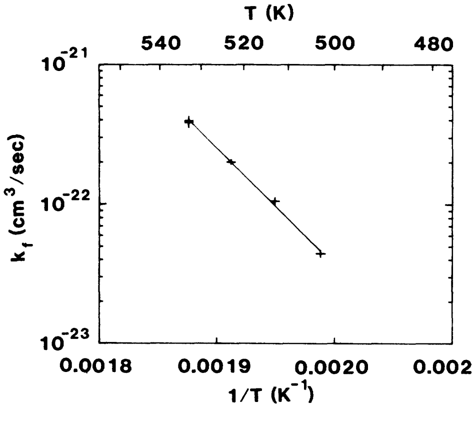

FIG. 9. Plot of the forward reaction rate, k_f, as a function of reciprocal absolute temperature. The data points correspond to the reaction rates deduced from the data in Figs. 1–5. The extent of the data symbols indicates the standard deviation in our measurements of k_f and T. These data are least-squares-fitted to the Arrhenius equation [Eq. (6)] and yield an activation energy of 1.66±0.06 eV and a preexponential factor, k_{0f}, of $1.94^{+2.00}_{-1.00}\times10^{-6}$ cm^3/sec.

of a H atom that could passivate a P_b center (see Sec. VI). In this case, k_f should increase with increasing oxide thickness for sufficiently thin oxides. The variation in k_{0f} as a function of oxide thickness is not consistent with either one of these effects by itself. Equation (2) suggests another possibility. In our analysis, $[H_2]$ is given by Eqs. (4) and (5); $[H_2]$ is not directly measured for each oxide. Thus, if there were an actual deviation in $[H_2]$ from the calculated value, then these variations in $[H_2]$ would cause a compensating deviation in k_f from its true value. Our results raise the possibility that the solubility of H_2 in thermal oxides may depend slightly on the oxidation process. Previous measurements by Shelby (see Fig. 9 of Ref. 33) suggests that variations in the solubility of H_2 among different types of vitreous silica are small.

VI. MODEL FOR PASSIVATION

It is possible to infer the likely nature of the dominant chemical reaction which is responsible for the passivation process in the temperature domain in which our measurements have been made. Chemical reactions which might reasonably occur are as follows:

$$P_b + H_2 \underset{b_1}{\overset{a_1}{\rightleftharpoons}} HP_b + H \ , \tag{7}$$

$$HP_b \underset{b_2}{\overset{a_2}{\rightleftharpoons}} P_b + H \ , \tag{8}$$

$$H_2 \underset{b_3}{\overset{a_3}{\rightleftharpoons}} H + H \ , \tag{9}$$

$$T + H_2 \underset{b_4}{\overset{a_4}{\rightleftharpoons}} HT + H \ , \tag{10}$$

and

$$HT \underset{b_5}{\overset{a_5}{\rightleftharpoons}} T + H \ , \tag{11}$$

In these chemical reactions HP_b represents a passivated P_b center and T represents a trap within the thermal oxide. This set of chemical reactions [Eqs. (7)–(11)] is not exhaustive. For example, these reactions are for neutral species, but charged species are conceivable. Also, there may be more than one kind of trap. The rates of H_2 dissociation would depend upon whether the H_2 molecule was dissociating in the thermal oxide or the silicon. Equations (7)–(11) list those possibilities which are considered in the following arguments. From the five chemical reactions listed above, it is not clear as to which chemical path the passivation process actually follows. We will consider three distinct chemical processes and formulate the corresponding rate equations.[37] We will attempt to identify the dominant chemical process by comparing the dependence of $[P_b]$ on time and H_2 concentration for each process with that observed experimentally.

Passivation process 1. In this process we imagine a two-step process. In the first step, atomic hydrogen is generated as a result of the dissociation of H_2 molecules [Eq. (9)]. This dissociation process might dominate either within the thermal oxide or at the Si-SiO_2 interface. The solubility of H_2 into crystalline silicon is negligible.[38] In the second step, some of the atomic hydrogen released in this process is captured by a P_b center, resulting in its passivation [Eq. (8)]; the balance of the atomic hydrogen is assumed to recombine [Eq. (9)] in this simple process. In this process it is assumed that the HP_b centers do not dissociate ($a_2=0$). The rate equations for this two-step process are a pair of coupled first-order nonlinear differential equations,

$$\frac{d[P_b]}{dt} = -b_2[H][P_b] \tag{12}$$

and

$$\frac{d[H]}{dt} = a_3[H_2] - b_3[H]^2 - b_2[H][P_b] \ , \tag{13}$$

which can be solved numerically for $[P_b]$ and [H] as a function of time. The H_2 concentration is, of course, known as a function of time. We have explored the solutions to these rate equations for various relative values of b_2, a_3, and b_3. In all of the solutions we explored, the decay in the number of P_b centers with time was nonexponential and the rate of decay in $[P_b]$ was not proportional to $[H_2]$ but closer to the square root of $[H_2]$. These features are significantly different from those we observe experimentally (Sec. V). Thus, the dominant mechanism for the passivation of P_b centers with H_2 does not proceed as a consequence of the dissociation of the H_2 molecule.

Passivation process 2. In this process H_2 molecules undergo partial chemical absorption at traps or misbondings, T, with the release of an atomic hydrogen [Eq. (10)]. This reaction supplies atomic hydrogen for reaction with P_b centers [Eq. (8)]. The balance of the atomic hydrogen is gettered by the traps or misbondings, T, in the SiO_2 [Eq. (11)]. We assume that in our temperature regime these three chemical reactions are irreversible ($a_2=b_4=a_5=0$) and that, at time $t=0$, $[H_2]$ goes from zero to a constant value. The rate equations for this process are

$$\frac{d[P_b]}{dt} = -b_2[H][P_b] \ , \tag{14}$$

$$\frac{d[T]}{dt} = -a_4[H_2][T] - b_5[H][T] \ , \tag{15}$$

and

$$\frac{d[H]}{dt} = a_4[H_2][T] - b_5[H][T] - b_2[H][P_b] \ . \tag{16}$$

Solutions for $[P_b]$, $[T]$, and [H] can be determined computationally using the method of finite differences. Although the decay in $[P_b]$ is typically nonexponential, the rate at which P_b centers decay is very nearly proportional to $[H_2]$. We are interested in solutions for which $[P_b]$ would also appear to decay exponentially. In order for this to occur, Eq. (14) demands that [H] be constant; therefore, we set $d[H]/dt$ in Eq. (16) equal to zero and solve for [H]:

$$[H]=\frac{a_4[H_2]}{b_5+b_2[P_b]/[T]} \, . \tag{17}$$

Substituting the solutions for $[P_b]$ and $[T]$ assuming [H] constant yields for [H] the expression

$$[H]=\frac{a_4[H_2]}{b_5+b_2\{[P_b(0)]/[T(0)]\}\exp\{(-b_2[H]+a_4[H_2]+b_5[H])t\}} \, . \tag{18}$$

This expression is time independent providing that the time-dependent exponential term is zero for all time. This constraint leads to the condition that

$$b_5=\frac{b_2}{2}\left[1-\frac{[P_b(0)]}{[T(0)]}\right] . \tag{19}$$

If Eqs. (14)–(16) are solved computationally with b_5 specified according to Eq. (19) by the values of b_2, $[P_b(0)]$, and $[T(0)]$, the time rate of change that has to occur in [H] is such that $[P_b]$ does decay nearly exponentially. The exponential character in the decay in $[P_b]$ is further enhanced if $a_4 \ll b_2$. Under these conditions the rate of decay in $[P_b]$ is approximately linearly proportional to the $[H_2]$ concentration.

Although a mathematical solution for which $[P_b]$ decays very nearly exponential is possible, the probability that such a physical process occurs appears unlikely. Such a solution appears unlikely because of the special relationship required [Eq. (19)] between two chemical reactions [Eq. (8) and (11)] that are physical independent. Furthermore, the relationship between b_2 and b_5 must be maintained as a function of temperature. Our computational solutions indicate that small nonexponential behavior necessarily occurs for times near zero; the data in Figs. 1–7 give no hint of nonlinearities in the exponential decay of $[P_b]$. Thus, passivation of P_b centers by this process is considered to be improbable.

Passivation process 3. In this process the H_2 reacts directly with the P_b center according to Eq. (7). Since the average separation between P_b centers is 50 Å,[3] the probability that the extra H atom is trapped at another P_b center is deemed negligible. This extra H atom can either readily escape from the oxide or become chemically bound within the oxide.[36] We assume in our temperature regime that this reaction [Eq. (7)] is irreversible ($b_1=0$); furthermore, the probability that the reverse reaction occurs is low due to the apparent scarcity of atomic hydrogen. The rate equation for this passivation process is very simply

$$\frac{d[P_b]}{dt}=-a_1[H_2][P_b] \, . \tag{20}$$

This rate equation agrees with our experimentally determined rate equation [Eq. (1)]. Thus, these considerations strongly suggest that the rate-limiting step in the passivation of the P_b center with H_2 is the chemical reaction in Eq. (7).

The measured value for k_{0f} is also consistent with passivation process 3. Let us assume that the H_2 molecule can diffuse to P_b centers as easily as any other accessible sites in the SiO_2. Thus, the fraction of time the H_2 molecule spends on the average at a P_b reaction site is, to a first approximation, the same as it spends in any of the accessible interstices in the SiO_2. The passivation reaction [Eq. (7)] occurs only while the H_2 molecule is in the vacant site adjacent to the P_b center; this vacant site is referred to as the reaction site. Consequently, the attempt frequency for the reaction, ν_s, is of the order of magnitude corresponding to the vibrational frequency of the H_2 molecule, 1.24×10^{14} Hz,[39] multiplied by the fraction of time, f, the H_2 molecule spends next to the P_b center. Thus, k_{0f} in Eqs. (6) is approximated by the expression

$$k_{0f}\sim\frac{\nu_s f}{[H_2]} \, , \tag{21}$$

which reduces to a strictly geometric term

$$k_{0f}\sim\frac{\nu_s}{V^{-1}} \, , \tag{22}$$

where V^{-1} is the density of accessible sites in vitreous SiO_2 and corresponds to 1.27×10^{21} interstices/cm^3.[30,33] This model predicts a k_{0f} on the order of 9.7×10^{-8} cm^3/sec. This is within approximately a factor of 20 for the measured value of k_{0f}. The details in the actual quantum process involving the chemical reaction in Eq. (7) are undoubtedly very complex. Thus, it may be an oversimplification to represent the rate of this quantum process by only the nearly-free-H_2 stretching frequency, ν_s. The order-of-magnitude agreement in k_{0f} which we have achieved between the measured and calculated passivation process 3 is perhaps not unreasonable.

Finally, since passivated P_b centers, HP_b, are observed to dissociate in vacuum at temperatures above 550 °C, the dissociation process which we observe is according to Eq. (8). Dissociation via the reverse reaction in Eq. (7) is highly improbable because the concentration of atomic hydrogen in our case is believed to be negligible; however, Griscom[40] has suggested that the reverse reaction in Eq. (7) might occur in a radiation environment that generates atomic hydrogen in the oxide. Johnson *et al.* have observed the passivation of P_b centers exposed with atomic hydrogen at temperatures as low as 125 °C;[41] their passivation process very likely corresponds to the reverse reaction in Eq. (8). One can observe atomic hydrogen with EPR in thermal oxides after low-temperature (<100 K) ionizing irradiation; however, atomic hydrogen in thermal oxides disappears as observed by EPR for temperatures above 100 K.[42]

VII. CONCLUSIONS

The molecular hydrogen chemistry of P_b centers is dominated by three thermochemical effects. The first is that P_b centers appear to be stable under vacuum annealing to temperatures of at least 850 °C. The second is that P_b centers can be passivated with molecular hydrogen; this reaction occurs for temperatures in excess of 220 °C. The third is that passivated P_b centers dissociate in vacuum for temperatures in excess of 550 °C.

In this paper we have measured the rate at which P_b centers are passivated in H_2 as a function of H_2 pressure and annealing time and temperature. The rate of passivation of P_b centers with H_2 is found to fit a kinetic model that is characterized by the rate equation in Eq. (1). According to this kinetic model the rate of passivation is proportional to the H_2 concentration and the density of P_b centers at the interface. The temperature dependence of k_f is found to be described by the Arrhenius equation [Eq. (6)] as evidenced by the data in Fig. 9. The kinetic parameters which characterize the passivation process are the activation energy, E_f, and the preexponential factor, k_{0f}, in Eq. (6). A least-squares fit of our experimentally determined values for k_f to the Arrhenius equation gives 1.66 ± 0.06 eV for the activation energy, E_f, and $1.94^{+2.00}_{-1.00}\times10^{-6}$ cm^3/sec for the preexponential factor, k_{0f}. These parameters are established for temperatures between 230 and 260 °C which correspond to a time-temperature domain where the rate of dissociation is negligible. This kinetic model appears valid for H_2 pressures ranging up to at least 760 Torr. The kinetic parameters which characterize the dissociation process are the subject of a forthcoming paper.

The rate at which P_b centers are passivated as indicated by Eq. (1) is consistent with a passivation process in which the H_2 molecule reacts directly with the P_b center (process 3, Sec. VI). The rate at which this reaction takes place is consistent with the diffusion of the H_2 molecule among the accessible interstices of the SiO_2 and the reaction site at the P_b center. We have also shown that the observed kinetics of passivation are inconsistent with a two-step chemical process in which H_2 molecules dissociate and the atomic hydrogen subsequently either passivates a P_b center or recombines to form H_2 (process 1, Sec. VI). In this case the rate of passivation of P_b centers is approximately proportional to the square root of the H_2 concentration, which is contrary to our experimental observations. We also argue that it is improbable that the process of passivation proceeds as a consequence of the partial absorption of H_2 at a trap or misbonding in the SiO_2 with the release of an atomic hydrogen atom which subsequently either passivates a P_b center or is captured in the SiO_2 (process 2, Sec. VI).

During the course of our experimental studies, we discovered that the spin-lattice relaxation rate of P_b centers at low temperatures (<100 K) is affected by the nature of the thermal oxide. In particular, the spin-lattice relaxation time, T_1, increases as the thickness of the thermal oxide is reduced below 800 Å. Increases in T_1 are very pronounced for annealing in H_2 between approximately 230 and 575 °C; also, thermal annealing in Ar gas increases T_1. The physical mechanisms responsible for these changes in T_1 are not yet understood.

ACKNOWLEDGMENTS

The extensive amount of sample preparation and technical support required for this study was provided by R. Shrouf. Appreciation is expressed to C. I. H. Ashby, D. K. Brice, R. C. Hughes, S. M. Myers, and H. J. Stein for many helpful suggestions and ideas concerning this work. This work is supported by the U.S. Department of Energy under Contract No. DE-AC04-76DP00789.

---

[1] O. L. Krivanek, D. C. Tsui, T. T. Sheng, and A. Kamgar, in *The Physics of SiO₂ and Its interfaces,* edited by S. T. Pantelides (Pergamon, New York, 1978), p. 356.

[2] J. H. Mazur, R. Gronsky, and J. Washburn, Proc. Soc. Photo-Opt. Instrum. Eng. **463**, 88 (1984).

[3] K. L. Brower and T. J. Headley, Phys. Rev. B **34**, 3610 (1986).

[4] A. Ourmazd, D. W. Taylor, J. A. Rentschler, and J. Bevk, Phys. Rev. Lett. **59**, 213 (1987).

[5] Y. Nishi, Jpn. J. Appl. Phys. **10**, 52 (1971).

[6] E. H. Poindexter, E. R. Ahlstrom, and P. J. Caplan, in *The Physics of SiO₂ and Its Interfaces,* Ref. 1, p. 227.

[7] E. H. Poindexter, Z. Phys. Chem. Neue Folge **151**, 165 (1987).

[8] K. L. Brower, Appl. Phys. Lett. **43**, 1111 (1983).

[9] K. L. Brower, Z. Phys. Chem. Neue Folge **151**, 177 (1987).

[10] E. H. Poindexter, G. J. Gerardi, M.-E. Rueckel, P. J. Caplan, N. M. Johnson, and D. K. Biegelsen, J. Appl. Phys. **56**, 2844 (1984).

[11] N. M. Johnson, D. K. Biegelsen, M. D. Moyer, S. T. Chang, E. H. Poindexter, and P. J. Caplan, Appl. Phys. Lett. **43**, 563 (1983).

[12] P. M. Lenahan and P. V. Dressendorfer, Appl. Phys. Lett. **41**, 542 (1982); **44**, 96 (1984); J. Appl. Phys. **55**, 3495 (1984).

[13] G. J. Gerardi, E. H. Poindexter, P. J. Caplan, and N. M. Johnson, Appl. Phys. Lett. **49**, 348 (1986).

[14] K. L. Brower, in *Materials Science Forum. Defects in Semiconductors I,* edited by H. J. von Bardeleben (Trans Tech, Aedersmansdorff, 1986), p. 181.

[15] A. Redondo, W. A. Goddard III, T. C. McGill, and G. T. Surratt, Solid State Commun. **20**, 733 (1976).

[16] M. Cook and C. T. White, Phys. Rev. Lett. **59**, 1741 (1987).

[17] A. H. Edwards, Phys. Rev. B **36**, 9638 (1987).

[18] S. J. Pearton, J. W. Corbett, and T. S. Shi, Appl. Phys. A **43**,

153 (1987).

[19] P. J. Caplan, E. H. Poindexter, B. E. Deal, and R. R. Razouk, J. Appl. Phys. **50**, 5847 (1979).

[20] N. M. Johnson, D. K. Biegelsen, and M. D. Moyer, J. Vac. Technol. **19**, 390 (1981).

[21] Our result is significantly different than that obtained by Johnson *et al.* (Ref. 11).

[22] Our white etch, which is an isotropic silicon etch, consisted of HF acid (80 ml), nitric acid (80 ml), acetic acid (280 ml), and acetic acid saturated with iodine (11 ml). This solution gives an silicon etch rate of 1000–2000 Å per 1 min. The etch rate is controlled by the amount of acetic acid. After etching, our samples were rinsed in deionized water and sonic cleaned in methanol.

[23] Our sample tube was pumped with an Alcatel turbomolecular pump bakced by an Alcatel mechanical vacuum pump. Initial pump down of the sample tube was achieved by "leaking" gas to the turbomolecular pump.

[24] All gases introduced into the sample tube are passed through individual filters consisting of a mixture of no. 13X molecular sieve and Drierite to remove residual oil and water.

[25] K. L. Brower, Rev. Sci. Instrum. **48**, 135 (1977).

[26] M. U. A. Bromba and H. Ziegler, Anal. Chem. **55**, 1299 (1983).

[27] G. D. Watkins, in *Materials Science Forum. Defects in Semiconductors III,* edited by H. J. von Bardeleben (Trans Tech, Aedermansdorff, 1986), p. 953.

[28] R. P. Vasquez, A. Madhukar, F. J. Grunthaner, and M. L. Naiman, J. Appl. Phys. **60**, 226 (1986).

[29] V. J. Kapoor and S. B. Bibyk, Thin Solid Films **78**, 193 (1981).

[30] J. F. Shackelford, P. L. Studt, and R. M. Fulrath, J. Appl. Phys. **43**, 1619 (1972).

[31] G. D. Watkins and J. W. Corbett, Phys. Rev. **138**, A543 (1965).

[32] K. L. Brower, Phys. Rev. B **5**, 4274 (1972).

[33] J. E. Shelby, J. Appl. Phys. **48**, 3387 (1977).

[34] J. E. Shelby, Phys. Rev. B **4**, 2681 (1971).

[35] J. F. Shackelford and J. S. Masaryk, J. Non-Cryst. Solids **21**, 55 (1976).

[36] S. M. Myers, J. Appl. Phys. **61**, 5428 (1987).

[37] S. W. Benson, *The Foundations of Chemical Kinetics* (McGraw-Hill, New York, 1966).

[38] A. van Wieringen and N. Warmoltz, Physica **22**, 849 (1956).

[39] J. Vitko, C. M. Hartwig, and P. L. Mattern, in *The Physics of SiO_2 and Its Interfaces,* Ref. 1, p. 215.

[40] D. L. Griscom, J. Appl. Phys. **58**, 2524 (1985).

[41] N. M. Johnson (private communication).

[42] K. L. Brower, P. M. Lenahan, and P. V. Dressendorfer, Appl. Phys. Lett. **41**, 251 (1982).